

# Short Paper: Hierarchical Underwater Acoustic Sensor Networks

Andrej Stefanov  
ECE Department  
Northeastern University  
Boston, MA, 02115  
a.stefanov@neu.edu

Milica Stojanovic  
ECE Department  
Northeastern University  
Boston, MA, 02115  
millitsa@mit.edu

## ABSTRACT

We propose a hierarchical underwater acoustic sensor network architecture in which the sensors and the collector stations operate in distinct layers. The hierarchical architecture is motivated by the property of the acoustic underwater transmission medium that for each transmission distance there exists an operating frequency for which the narrow-band signal-to-noise ratio is maximized. The sensors and collector stations are consequently allocated different operating frequencies. We assume a uniform distribution of both sensors and collector stations over the finite area of the sensing field. The node-to-node channel is modeled using frequency dependent path loss and Ricean fading. We adopt a communication theoretic approach and study the interdependence of the sustainable number of hops through the network, end-to-end frame error probability, power and bandwidth allocation. The analysis is performed under the assumption that there is interference from other nodes within the same layer of the hierarchy. We present numerical examples that illustrate the network performance and demonstrate that there are preferred operating frequencies which ensure network operation without any cross-interference between the collector network and the sensor network.

## Categories and Subject Descriptors

H.4 [Information Systems Applications]: Networks and communication theory

## General Terms

Theory, Design, Performance

## Keywords

Underwater acoustic networks, hierarchical sensor networks, connectivity

Permission to make digital or hard copies of all or part of this work for personal or classroom use is granted without fee provided that copies are not made or distributed for profit or commercial advantage and that copies bear this notice and the full citation on the first page. To copy otherwise, to republish, to post on servers or to redistribute to lists, requires prior specific permission and/or a fee.

WUWNet'10, Sept. 30 - Oct. 1, 2010, Woods Hole, Massachusetts, USA  
Copyright 2010 ACM 978-1-4503-0402-3 ...\$10.00.

## 1. HIERARCHICAL SENSOR NETWORK

We introduce a hierarchical sensor network architecture. It is motivated by the frequency-distance dependence property of underwater acoustic systems. The bottom mounted sensors constitute the first layer in the architecture. The sensors are organized into disjoint cells, as illustrated in Figures 2 and 3. The sensors in each cell communicate their information utilizing multihop relaying to the collector station located at the center of the cell. The collector stations (collectors), which are also bottom mounted, form the second layer in the hierarchical architecture. The collector stations also utilize multihop relaying to transmit their respective information to the central collector.

We adopt a communication theoretic framework [1], and investigate the network performance in the presence of interference from other nodes within the same layer of the hierarchy, focusing on the interdependence between the sustainable number of hops in the network, as an indicator of network connectivity; end-to-end frame error probability, power and bandwidth allocation.

### 1.1 Underwater Acoustic Propagation

Attenuation, or path loss, that occurs in an underwater acoustic channel over a distance  $d$  for a signal of frequency  $f$ , is given by  $A(d, f) = A_0 d^\kappa a(f)^d$ , where  $A_0$  is a unit-normalizing constant,  $a(f)$  is the absorption coefficient and  $\kappa$  is the spreading factor. In the case of practical spreading,  $\kappa = 1.5$ . The absorption coefficient, which is an increasing function of frequency, can be expressed empirically using Thorp's formula [2]. The ambient noise in the ocean comes from diverse sources, (turbulence, shipping, waves and thermal noise), which can be described by Gaussian statistics and a continuous power spectral density [2].

### 1.2 Data Gathering Protocol

Both the sensors and the collectors utilize the same data gathering protocol. We consider two versions of the protocol and describe it in terms of sensor-to-sensor transmissions to the collector.

*Protocol 1:* The protocol is illustrated in Figure 1. The sensors closest to the collector transmit their information first in a single-hop transmission to the collector. The sensors that are two hops away transmit next through a two-hop route to the collector and so on. As they need to relay the data, the sensors closer to the collector can take advantage of the established route and transmit again. For example, Figure 1 shows sensors that are three hops away from the collector. They establish three-hop routes. The other sen-

sors in the route, that are within two hops and a single hop from the collector, take advantage of the established route and send new information to the collector.

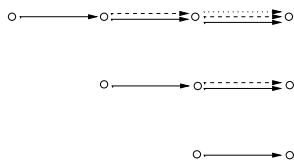


**Figure 1: Data gathering protocol.**

We note that spatial reuse of the bandwidth is possible, so that there can exist multiple routes to the same collector. Of course, this leads to interference among transmissions utilizing the same time slot and the same bandwidth.

*Protocol 2:* The second data gathering protocol is a simplified version of the protocol described above. In this case, the sensors still utilize multihop transmissions; however, all sensors that are within the collector’s cell transmit only once to the collector. In other words, sensors closer to the collector that are part of a multihop route for a sensor that is farther away from the collector only act as relays and do not transmit new information to the collector.

### 1.3 Collector Network Topology

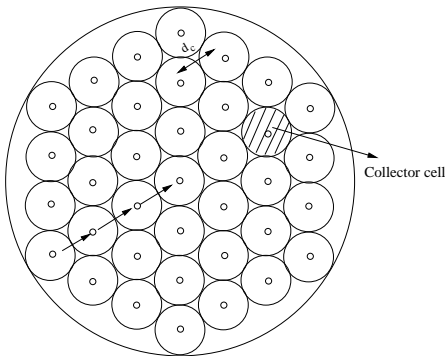


**Figure 2: Network of collector stations.**

We consider a network of bottom mounted collector stations. Therefore, we focus on a two dimensional network that provides coverage over a certain area. Let the area of the network be a circle of radius  $r$ . We assume a uniform distribution of collector stations in the network as depicted in Figure 2. Given the number of collector stations in the network,  $K$ , and the area of the network,  $\mathcal{A}$ , the density of the collector stations in the network,  $\rho_c$ , is

$$\rho_c = \frac{K}{\mathcal{A}}. \quad (1)$$

For a uniform collector station distribution, the distance between the collector stations,  $d_c$ , is

$$d_c = \frac{c}{\sqrt{\rho_c}} \quad (2)$$

where  $c$  is a constant that depends on the node placement (grid pattern). Without loss of generality we assume that  $c = 1$ .

We assume multihop transmission based on nearest neighbor routing. This is an energy saving strategy, and as such it

may be attractive for networks with limited energy, battery-powered nodes. As the longest multihop route in the network is along the radius of the network  $r$ , the maximum number of collector-to-collector hops is

$$n_c^{\max} = \frac{r}{d_c} = \frac{\sqrt{\mathcal{A}/\pi}}{\sqrt{\mathcal{A}/K}} = \sqrt{\frac{K}{\pi}}. \quad (3)$$

Let the average number of hops for a multihop route across collector stations be denoted as  $\bar{n}_c$ . Then, given the data gathering protocol, we have

$$\bar{n}_c \lesssim \delta n_c^{\max} = \delta \sqrt{\frac{K}{\pi}} \quad (4)$$

where  $\delta$  is a constant that depends on the data gathering protocol. For example, in the case of protocol 1,  $\delta = \frac{1}{2}$ ; in the case of protocol 2,  $\delta = \frac{2}{3}$ .

### 1.4 Sensor Network Topology

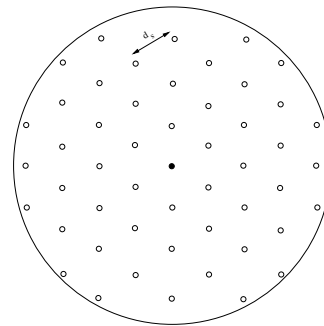


**Figure 3: A collector cell contains  $N_c = \frac{N}{K}$  sensors.**

We consider a network of bottom mounted sensors. We assume a uniform distribution of  $N$  sensors in the network. As there are  $K$  collector stations there are  $N_c = \frac{N}{K}$  sensors per collector station, as depicted in Figure 3. The coverage area (cell) of each collector is  $\mathcal{A}_c$ . Hence, the density of the sensors,  $\rho_s$ , is

$$\rho_s = \frac{N_c}{\mathcal{A}_c} = \frac{N}{K\mathcal{A}_c} = \frac{N}{\mathcal{A}} = \frac{1}{d_s^2}. \quad (5)$$

Following the steps of Section 1.3, we obtain the maximum and the average number of sensor-to-sensor hops, respectively as

$$n_s^{\max} = \frac{1}{\sqrt{\pi}} \sqrt{\frac{N}{K}} \quad (6)$$

$$\bar{n}_s \lesssim \frac{\delta}{\sqrt{\pi}} \sqrt{\frac{N}{K}}. \quad (7)$$

### 1.5 Interference Model

In order to illustrate the effect of interference, we focus on a single transmission from a source node to a destination node, as depicted in Figure 4. We impose a protocol constraint: no nodes that are at the same distance from the destination node as the source node are allowed to transmit in the same time slot and in the same frequency band as the source during the source node’s transmission. The remaining nodes that may interfere with the source’s transmission

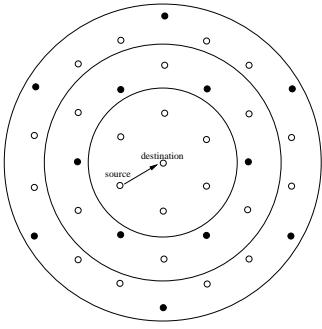


Figure 4: Interfering nodes in the network.

are organized in tiers. Assuming a hexagonal grid as an approximation of the network topology, there will be at most 12 interfering nodes in tier 1, 18 interfering nodes in tier 2, etc. A scenario where all the nodes in the network transmit at the same time is unrealistic, as some nodes will be receiving while others transmit. Figure 4 depicts a scenario where half of the nodes in tier 1 and a third of the nodes in tier 2 transmit at the same time and in the same frequency band as the source, therefore creating interference. Assuming that all the nodes transmit with some constant power spectral density (p.s.d.)  $S$ , the combined interference from the nodes in the first and second tier is

$$I(f) \approx \frac{c_1 S}{A(2d, f)} + \frac{c_2 S}{A(3d, f)} \quad (8)$$

where  $c_1 \leq 12$  and  $c_2 \leq 18$  are constants indicating the number of interfering nodes in tiers 1 and 2, respectively. In the example presented in Figure 4, we have  $c_1 = c_2 = 6$ . As there are multiple interfering nodes in the network, we assume that the interference is Gaussian with p.s.d.  $I(f)$ . Using the attenuation  $A(d, f)$ , the noise p.s.d.  $N(f)$  and the interference p.s.d.  $I(f)$ , we can evaluate the narrowband signal to interference plus noise ratio (SINR) observed over a distance  $d$ , as shown in Figure 5 (LHS). We observe that there is a preferred operating frequency,  $f_o(d)$ , which depends on the distance,  $d$ . The factor  $[A(d, f)(N(f) + I(f))]^{-1}$  is maximized at this frequency. Figure 5 (RHS) presents this preferred operating frequency as a function of the distance, given a transmit p.s.d. level of  $S = 150$  dB re  $\mu$  Pa per Hz for  $f$  in kHz.

## 1.6 Multihop Transmission

We assume that both the sensor network and the network of collector stations utilize uncoded BPSK transmission with a simple demodulate-and-forward strategy employed by the relays. The end-to-end frame error probability (FEP) for a multihop route with  $n_h$  hops is given by

$$p_{\text{route}} = 1 - (1 - p_b)^{L n_h} \quad (9)$$

where  $p_b$  denotes the bit error probability of a single node-to-node link, and  $L$  denotes the frame size in bits.

We consider the quality-of-service for the network in terms of the maximum allowed end-to-end route frame error probability, i.e., we require that  $p_{\text{route}} \leq p_{\text{route}}^{\max}$ .

Let the number of hops that can be sustained by the network, i.e., the number of hops that can satisfy the maximum end-to-end route frame error probability, be denoted by  $n_{\text{sh}}$ .

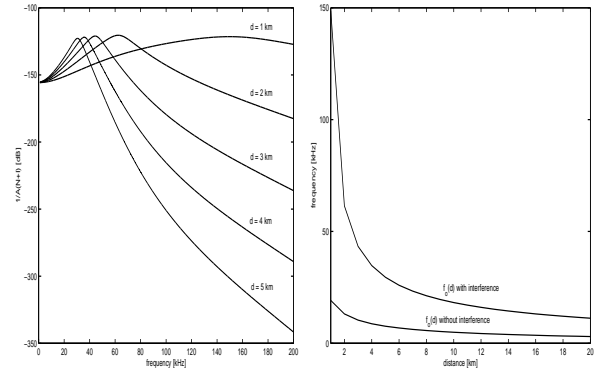


Figure 5: (LHS) The narrowband signal to noise plus interference ratio for various distances  $d$ . (RHS) Operating frequency  $f_o(d)$ . The transmit power spectral density is  $S = 150$  dB re  $\mu$  Pa per Hz. The spreading factor is  $\kappa = 1.5$ .

From Eq. (9), it follows that  $n_{\text{sh}}$  can be calculated as<sup>1</sup>

$$n_{\text{sh}} = \frac{1}{L} \frac{\log(1 - p_{\text{route}}^{\max})}{\log(1 - p_b)} \approx \frac{1}{L} \frac{p_{\text{route}}^{\max}}{p_b}. \quad (10)$$

We focus on a frequency non-selective Ricean fading model for the node-to-node channel [3]. Under the assumption that perfect channel state information is available at the receiver, the bit error probability,  $p_b$ , can be upper bounded as [4]

$$p_b \leq \frac{1 + \mathcal{K}}{1 + \mathcal{K} + \gamma(d, f)} \exp\left(-\frac{\mathcal{K}\gamma(d, f)}{1 + \mathcal{K} + \gamma(d, f)}\right) \quad (11)$$

where  $\mathcal{K}$  denotes the Ricean fading factor and  $\gamma$  denotes the SINR. We assume that the attenuation, noise and interference are constant over the operational bandwidth  $B$ , so that the SINR can be calculated at the operating frequency  $f_o(d)$  as

$$\gamma(d, f_o) = \frac{P}{A(d, f_o)(N(f_o) + I(f_o))B}. \quad (12)$$

The frequency-nonselctive assumption is a suitable approximation for systems with narrow bandwidth. It can also be extended to wideband multi-carrier systems, such as OFDM. In that case, the operating frequency,  $f_o(d)$ , would describe the performance on one of the carriers. The performance on the other carriers would correspond to the frequency  $f_o(d)$  shifted by multiples of subcarrier separation  $\Delta f$ .

## 2. NUMERICAL EXAMPLES

We present numerical examples to examine the relationship between the sustainable number of hops, the end-to-end frame error probability, signal power and bandwidth. We assume Ricean fading for each node-to-node channel. The Ricean fading factor is taken to be  $\mathcal{K} = 10$ . We consider a maximum allowed end-to-end FEP of  $10^{-3}$  for both the collector and the sensor networks. The acoustic power levels are expressed in dB re  $\mu$  Pa. We neglect any fixed losses. Inclusion of additional frequency independent losses, and an

<sup>1</sup>Note that while the analysis does not consider it explicitly, in practice  $\{n_{\text{sh}}, n_c^{\max}, n_s^{\max}\} \in \mathbb{N}$ .

adjustment of the background noise level to suit a particular environment and provide the necessary SINR margins, will scale the results in absolute value, for the power, as well as the operating frequency (toward lower values commonly found in practice), but will not alter the general behavior. The frame size is  $L = 1000$  bits. We assume that the hierarchical sensor network utilizes the data gathering protocol 1. Hence, the average number of collector-to-collector hops,  $\bar{n}_c$ , and sensor-to-sensor hops,  $\bar{n}_s$ , are calculated for  $\delta = \frac{1}{2}$ . The spreading factor is  $\kappa = 1.5$ , the shipping activity factor is  $s = 0.5$  and the wind speed is  $w = 0$  m/s.

We present an example of a sensor network with 10000 sensors and 200 collectors deployed uniformly over a circular network of area  $\mathcal{A} = 10000$  km<sup>2</sup>. Hence, there are  $N_c = 50$  sensors per collector station. Each collector's coverage area is  $\mathcal{A}_c \approx 50$  km<sup>2</sup>. The performance of the network of collector stations is presented in Figure 6. The collector's initial transmit power is  $P_c = 173$  dB re  $\mu$  Pa and the bandwidth is  $B_c = 4$  kHz. The corresponding performance of each collector's cell sensor network is presented in Figure 7. The sensor's initial transmit power is  $P_s = 170$  dB re  $\mu$  Pa and the bandwidth is  $B_s = 4$  kHz. We assume that the collector stations and the sensors have the ability to adjust their power levels, so that the sustainable number of hops through the network never exceeds the maximum number of hops given in Eqs. (3) and (6), respectively. The Figures present the sustainable number of hops, operating frequency and transmit power. We require the sustainable number of hops to be equal to the maximum number of hops in order to guarantee full connectivity. As we observe from Figures 6 and 7, this is the case for both the network of collector stations and the sensor network. We also observe that the operating frequency for the network of collector stations is different from the operating frequency for the sensor network. For example, the operating frequency for the network of collector stations when the number of collectors is  $K = 200$  is  $f_o(d_c) = 27$  kHz. The operating frequency for the sensor network when the number of sensors per collector cell is  $N_c = 50$  is  $f_o(d_s) = 190$  kHz. Hence, there is a sufficient frequency separation to ensure the operation of the hierarchical sensor network without any cross-interference between the collector network and the sensor network.

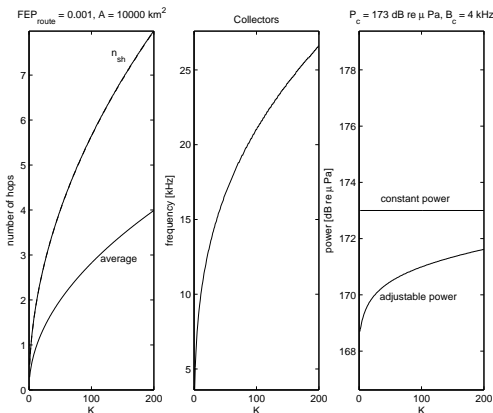


**Figure 6: Sustainable number of hops for a uniform network of collector stations with Ricean fading, operating frequency and transmit power, the bandwidth is  $B_c = 4$  kHz.**

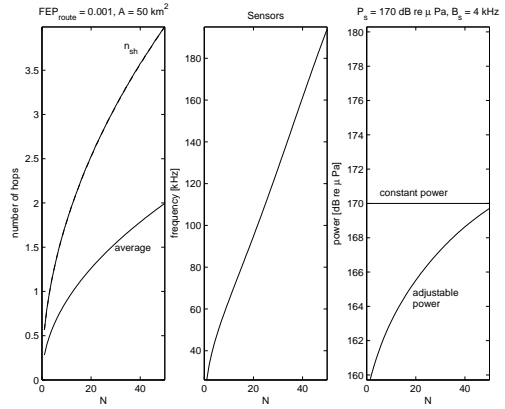


**Figure 7: Sustainable number of hops for a uniform distribution of sensors in a collector cell with Ricean fading, operating frequency and transmit power, the bandwidth is  $B_s = 4$  kHz.**

### 3. CONCLUSIONS

We considered a hierarchical sensor network architecture where the sensors and the collector stations operate in distinct layers. The hierarchical architecture was motivated by the property of the acoustic underwater transmission medium that for each transmission distance there exists an operating frequency for which the narrow-band SINR is maximized. We assumed a uniform distribution of both the sensors and the collectors over the finite area of the sensing field. A communication theoretic analysis conducted under the assumption of multihop transmission and Ricean fading for each node-to-node channel revealed the interdependence of the sustainable number of hops through the network, end-to-end frame error probability, power and bandwidth allocation. Numerical examples showed that there is a sufficient frequency separation to ensure the operation of the hierarchical sensor network without any cross-interference between the collector network and the sensor network.

### 4. ACKNOWLEDGMENTS

This work was supported in part by the NSF grant 0831728 and the ONR grant N00014-09-1-0700.

### 5. REFERENCES

- [1] O. Tonguz and G. Ferrari. *Ad-Hoc Wireless Networks: A Communication Theoretic Perspective*. Wiley, 2006.
- [2] M. Stojanovic and J. Preisig. Underwater acoustic communication channels: Propagation models and statistical characterization. *IEEE Communications Magazine*, pages 84–89, January 2009.
- [3] P. Qarabaqi and M. Stojanovic. Statistical modeling of a shallow water acoustic communication channel. In *Proc. Underwater Acoustic Measurements Conference*, June 2009.
- [4] S. Benedetto and E. Biglieri. *Principles of Digital Transmission with Wireless Applications*. Kluwer/Plenum, 1999.